Computers & Fluids 77 (2013) 152–158

Contents lists available at SciVerse ScienceDirect

Computers & Fluids

journal homepage: www.elsevier.com/locate/compfluid

Direct numerical simulation of an oscillating droplet in partial contact with a substrate

Ufuk Olgac [1], Daulet Izbassarov, Metin Muradoglu *

Department of Mechanical Engineering, Koç University, Rumelifeneri Yolu, 34450 Sariyer, Istanbul, Turkey

ARTICLE INFO

Article history:
Received 5 September 2012
Received in revised form 4 January 2013
Accepted 4 March 2013
Available online 21 March 2013

Keywords:
Drop oscillation
Interfacial flows
Front-tracking method
Direct numerical simulation

ABSTRACT

Small-amplitude oscillations of a viscous drop that is in a partial contact with a flat substrate are investigated computationally using a finite-difference/front-tracking method. Emphasis is placed on the first mode resonance frequency response of the droplet for a wide range of contact angles. It is found that numerical results converge to the theoretical predictions of Strani and Sabetta (Strani M, Sabetta F. J Fluid Mech 1984;141:223–47) for high contact angles, whereas considerable discrepancy is observed as contact angle decreases. However, the dependence of the frequency on the drop radius, drop density and surface tension coefficient remains the same as predicted by the Strani and Sabetta theory. It is also found that the effects of density and viscosity ratio become insignificant for the density and viscosity ratios larger than 10. The oscillations are found to be damped exponentially in time due to viscous dissipation similar to the case of an isolated droplet and the damping rate decreases with increasing contact angle.

1. Introduction

The free vibration of a liquid drop in partial contact with a solid surface has received significant interest due to a range of applications including crystal-growth in space [20,3], ink-jet printing [2], liquid lenses [14] and superhydrophobic surfaces [10]. Motivated by the experimental studies of Rodot et al. [20] and Bisch et al. [3], Strani and Sabetta theoretically analyzed the small-amplitude oscillations of a sessile drop in partial contact with a spherical bowl for both inviscid [23] and viscous [24] cases as an approximation to the free vibration of a droplet on a solid substrate. They found that there exists an additional low-frequency vibrational mode ($n = 1$) for supported drops compared to the isolated drops where it is zero. The lowest axisymmetric oscillation frequency predicted by the Strani and Sabetta [23] theory is given by

$$\omega_{SS} = (2\pi)^{-1}\sqrt{\frac{\gamma}{\rho_i R^3 \lambda_1(\theta_c)}}, \tag{1}$$

where γ is the surface tension coefficient, ρ_i is the density of the droplet, R is the radius of the undisturbed droplet (Fig. 1) and λ_1 is the eigenvalue associated with the lowest frequency mode ($n = 1$) that depends on the contact angle θ_c and the density ratio of droplet and ambient fluids. Strani and Sabetta [23] calculated resonance frequencies for various contact angles and found a good agreement with the experimental results of Bisch et al. [3] for high contact angles, i.e., $\theta_c > 150°$. However, they also found that the theory generally over predicts the frequency response of the constrained droplet and the discrepancy increases as the contact angle decreases. They later extended the inviscid theory to include the viscous effects and found out only a weak influence of viscosity on oscillation frequency which becomes progressively weaker as contact angle decreases [24].

On the computational side, Foote [5] used an extension of the Marker-and-Cell method to investigate the small and large amplitude oscillations of a freely vibrating drop. Basaran [1] used a Galerkin/finite-element technique to simulate the moderate-to-large amplitude axisymmetric oscillations of a liquid drop and found consistent results with Prosperetti's [16] linear predictions for small-to-moderate-amplitude oscillations and Foote's [5] predictions for large-amplitude oscillations. Later, using the same method, Basaran and DePaoli [2] studied the nonlinear oscillations of pendant drops from a solid rod that are surrounded by an ambient gas. They reported results on the effects of drop size, fluid properties and initial deformation, which was extended to forced oscillations of pendant drops by Wilkes and Basaran [30]. James et al. [8] used a volume-of-fluid (VOF) method to simulate forced vibration of a sessile droplet on a vertically vibrating solid substrate. They were able to capture the interfacial breakup as well as the subsequent ejection of a smaller droplet. Note that the same problem has also been studied experimentally by James et al. [9] and Vukasinovic et al. [29]. More recently, Ramalingam and Basaran [18] examined axisymmetric oscillations of a double droplet system (DDS) consisting of a sessile and a pendant drop that are coupled through a liquid filled cylindrical hole in a plate using a

* Corresponding author. Tel.: +90 (212) 338 14 73; fax: +90 (212) 338 15 48.
E-mail address: mmuradoglu@ku.edu.tr (M. Muradoglu).
[1] Current address: The Interface Group, Institute of Physiology, University of Zurich, Winterthurerstrasse 190, CH-8057, Switzerland.

0045-7930/$ - see front matter © 2013 Elsevier Ltd. All rights reserved.
http://dx.doi.org/10.1016/j.compfluid.2013.03.007

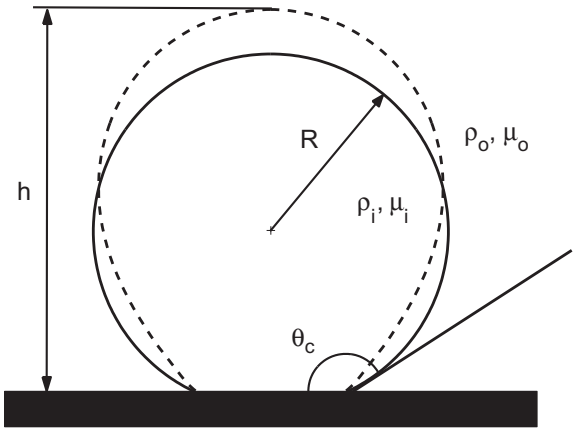

Fig. 1. Definition sketch. The solid and dashed lines represent the equilibrium and perturbed shapes, respectively, for the axisymmetric mode of vibration ($n = 1$).

Galerkin/finite-element method to determine the modal shapes and modal frequencies of capillary switches. They found that, while a single pendant (sessile) drop has one additional oscillation mode compared to a free drop, a DDS exhibits roughly twice as many oscillation modes as a pendant (sessile) drop.

Siekmann and Schilling [22] performed boundary element simulations and confirmed the Strani and Sabetta theory for the free vibration of a droplet in partial contact with a rigid spherical cavity. Ganan and Barrero [6] computationally studied the small amplitude oscillations of a captive drop that is in partial contact with a flat substrate using an analytical spectral method. They found that the computational results are in a reasonable agreement with the Strani and Sabetta theory for large contact angles. Bostwick and Steen [4] considered a similar problem and studied the free vibration of a liquid droplet that is pinned on a circle of contact using a spectral method. They found that the pinning of droplet introduces a new low-frequency mode similar to the linear oscillations of a drop in partial contact with a spherical bowl. The same problem has been also studied by Prosperetti [17] using a different approach that considerably simplifies the solution procedure but the results are essentially the same as those of Bostwick and Steen [4]. Ramalingam et al. [19] have more recently studied the same problem using two separate analytical solution procedures and showed some differences in the vicinity of the contact point compared to the results of Bostwick and Steen [4].

The Strani and Sabetta theory has recently been utilized in several experimental studies for various purposes such as measuring contact angle [31,10,11], examining the effects of excitation signal on the stable contact angle [21], and estimating size of sessile droplets and their evaporation kinetics [26]. Here we draw inspiration from a particular set of experimental study performed by Jonas et al. [10] who used the Strani and Sabeta theory to deduce the contact angle of micro-droplet on a superhydrophobic substrate from the measured resonance oscillation frequency of the droplets. When the density of the ambient fluid is much smaller than that of the droplet, the effects of density ratio become negligible and thus λ_1 in Eq. (1) is just function of the contact angle. Based on this observation, Jonas et al. [10] determined contact angles of sessile droplets on superhydrophobic surfaces by examining the vibrational resonances driven by the surface oscillations. The accuracy of the measured contact angle is mainly determined by the validity of the Strani and Sabetta theory since the resonance frequencies are measured very precisely. They reported that the deduced contact angles are consistently higher than those measured using conventional methods for larger droplets on the same superhydrophobic surface.

The present study is motivated by the increased use of Strani and Sabetta theory in experimental measurements and aims to assess the validity of the Strani and Sabetta theory and fully characterize the problem for the range of contact angles between 90° and 180°. For this purpose, axisymmetric vibrations of a droplet that is in partial contact with a flat substrate are studied computationally using a direct numerical simulation within the framework of a finite-difference/front-tracking method [28,15,25]. The computational results are compared with the available experimental data as well as with the Strani and Sabetta theory.

2. Problem statement, formulation and numerical method

We consider an axisymmetric liquid droplet of radius R that sits on a flat substrate with a fixed contact angle of θ_c as sketched in Fig. 1. The density and viscosity of the droplet and ambient fluids are ρ_i, μ_i and ρ_o, μ_o, respectively, and the surface tension is γ. Note that the properties of the droplet and ambient fluids are denoted by subscripts i and o, respectively. The height of droplet measured from the substrate is denoted by h and is used to monitor the surface oscillations. The drop interface is initially perturbed using the first mode shape obtained from the Strani and Sabetta [23] theory. The droplet starts vibrating from the quiescent initial conditions. Considering the experimental conditions of Bisch et al. [3] and Jonas et al. [10], we assume that the contact line remains fixed at the equilibrium position and the effects of gravity are negligible.

The fluid motion is assumed to be governed by the incompressible Navier–Stokes equations which are solved inside and outside of the droplet using a front-tracking method [28,15,25]. Following Unverdi and Tryggvason [28], a single set of governing equations can be written for the entire computational domain as long as the jumps in material properties are treated correctly and the effects of surface tension are included. Assuming that the flow is axisymmetric, the Navier–Stokes equations can be written in the framework of the front-tracking method as

$$\begin{aligned}
&\frac{\partial \rho v_r}{\partial t}+\frac{1}{r}\frac{\partial r\rho v_r^2}{\partial r}+\frac{\partial \rho v_r v_z}{\partial z}=-\frac{\partial p}{\partial r}+\frac{\partial}{\partial r}\left(2\mu\frac{\partial v_r}{\partial r}\right)+2\mu\frac{\partial}{\partial r}\left(\frac{v_r}{r}\right)\\
&\quad+\frac{\partial}{\partial z}\mu\left(\frac{\partial v_z}{\partial r}+\frac{\partial v_r}{\partial z}\right)-\int_A \gamma\kappa\mathbf{n}\delta(\mathbf{x}-\mathbf{x_f})dA\cdot\hat{\mathbf{i}}_r,\\
&\frac{\partial \rho v_z}{\partial t}+\frac{1}{r}\frac{\partial r\rho v_r v_z}{\partial r}+\frac{\partial \rho v_z^2}{\partial z}=-\frac{\partial p}{\partial z}+\frac{1}{r}\frac{\partial}{\partial r}\mu r\left(\frac{\partial v_z}{\partial r}+\frac{\partial v_r}{\partial z}\right)\\
&\quad+\frac{\partial}{\partial z}\left(2\mu\frac{\partial v_z}{\partial z}\right)-\int_A \gamma\kappa\mathbf{n}\delta(\mathbf{x}-\mathbf{x_f})dA\cdot\hat{\mathbf{i}}_z,
\end{aligned}\tag{2}$$

where v_r and v_z are the velocity components in the radial and axial directions, respectively, p is the pressure, ρ and μ are the discontinuous density and viscosity fields, respectively. The effect of surface tension is included as a body force in the last term on the right hand side of Eq. (2), where γ is the surface tension, κ is twice the mean curvature, and $\mathbf{n}$ is a unit vector normal to the interface with components of $\hat{\mathbf{i}}_r$ and $\hat{\mathbf{i}}_z$ in the radial and axial directions, respectively. The surface tension acts only on the interface as indicated by the three-dimensional delta function δ, whose arguments $\mathbf{x}$ and $\mathbf{x}_f$ are the points at which the equation is evaluated and a point at the interface, respectively. The Navier–Stokes equations are solved together with the incompressible continuity equation

$$\frac{\partial r v_r}{\partial r}+\frac{\partial r v_z}{\partial z}=0.\tag{3}$$

It is also assumed that the material properties such as density and viscosity remain constant following a fluid particle, i.e., $D\rho/Dt = 0$ and $D\mu/Dt = 0$, where D/Dt denotes the substantial derivative. Density and viscosity vary discontinuously across the interface and are

specified based on the indicator function as $\rho = \rho_i I + (1 - I)\rho_o$ and $\mu = \mu_i I + (1 - I)\mu_o$, respectively. The indicator function I is defined such that it is unity inside the droplet and zero outside. The indicator function is computed using the standard procedure as described by Tryggvason et al. [27].

The flow equations are solved using the finite-difference/front-tracking method developed by Unverdi and Tryggvason [28]. The front-tracking method has been extended to treat the moving contact lines by Muradoglu and Tasoglu [15] and successfully applied to model the single cell epitaxy by Tasoglu et al. [25]. Note that, although the treatment of moving contact line is readily available in the present numerical method, we consider only the case of fixed contact line since we are mainly interested in small amplitude oscillations in the present study. It is emphasized here that, for small amplitude oscillations, the deviation of the apparent contact angle from the static contact angle is well within the experimental uncertainties involved in the experimental correlations (e.g., Kistler's correlation [13]) that are usually employed to relate the apparent contact angle to the static contact angle and the contact line capillary number. It has been thus preferred to use the fixed contact angle in all the results presented in this paper. The flow equations are solved using a uniform Cartesian grid with a projection method. The momentum and continuity equations are discretized using second-order central difference approximation for the spatial derivatives and an explicit second-order predictor–corrector method for time integration. The discretized equations are solved on a fixed staggered grid using the Marker-and-Cell method of Harlow and Welch [7]. No slip and axis of symmetry boundary conditions are applied on the substrate and at the symmetry line, respectively. Far-field (or full slip) boundary conditions are applied at the lateral and top boundaries. Note that the influence of boundary treatment is found to be negligible even when no-slip boundary conditions are used for these boundaries provided that the boundaries are sufficiently remote from the droplet, e.g., for the computational domain employed here.

The governing non-dimensional numbers are the Bond number $Bo = g(\rho_i - \rho_o)R^2/\gamma$ where g is the gravitational acceleration, the Ohnesorge number $Oh = \mu_i/\sqrt{\rho_i \gamma R}$, the contact angle θ_c, density ratio ρ_i/ρ_o and viscosity ratio μ_i/μ_o. The Bond number represents the gravitational forces relative to the interfacial forces while the Ohnesorge number measures the relative importance of the viscosity of drop and surface tension. Gravitational effects are neglected in this study since $Bo \ll 1$ in the experimental study of Jonas et al. [10] as well as in Rodot et al. [20] and Bisch et al. [3]. For a typical liquid–gas system (e.g., silicone oil droplet in air), density and viscosity ratios are of the order of 1000 and 100. However all computations are performed for much smaller density and viscosity ratios to simulate a liquid–gas system, i.e., $\rho_i/\rho_o = 10$ and $\mu_i/\mu_o = 10$ in the present study mainly due to numerical considerations, i.e., convergence rate of pressure Poission solver deteriorates significantly when the density and viscosity ratios are much greater than 10. Note that the effects of viscosity and density ratios are expected to be small when $\rho_i/\rho_o \geqslant 10$ and $\mu_i/\mu_o \geqslant 10$ for the kind of problems as studied here [15,25]. In addition, some further computations are performed here to confirm the validity of this assumption as will be discussed in the results section below.

3. Results and discussion

Extensive computational simulations are performed to examine the validity of Strani and Sabetta theory [23] and fully characterize the small amplitude vibration of a micro-droplet in partial contact with a flat solid substrate. The flow equations are solved in their dimensional forms but the results are presented in terms of relevant dimensionless quantities. The computational domain extends $2.5R$ in the radial direction and $3.75R$ in the axial direction. Computations are first performed to show the grid convergence as briefly discussed in the Appendix. We've found that it is sufficient to use a uniform Cartesian grid containing 384×576 grid points in the axial and radial directions, respectively, to reduce the spatial discretization error below 1%. We thus employed this grid in all the computational results reported here. The present numerical method is explicit so the time step is restricted to maintain numerical stability. In the present study, the restrictions due to convection, viscosity and surface tension are taken into account and the time step is thus determined by $\Delta t = \min\left(\frac{\Delta x^2}{4\eta}, \frac{\Delta x}{|U|}, \sqrt{\frac{(\rho_o+\rho_i)\Delta x^3}{4\pi\gamma}}\right)$ where Δx is the grid spacing, η is the kinematic viscosity and $|U|$ is the magnitude of the velocity. Note that, although not shown here due to space considerations, the time stepping error is negligible compared to the spatial discretization error in all the results presented in this paper.

First the results are presented in this section to show the accuracy of the numerical method. For this purpose, simulations were performed for the case studied experimentally by Bisch et al. [3]. The material properties are taken from Strani and Sabetta [24] and are specified as $\rho_i = \rho_o = 1000$ kg/m^3, $\mu_i = 0.005$ kg/(m s), $\mu_o = 0.0014$ kg/(m s), $\gamma = 0.037$ N/m and $R = 4.44$ cm. Simulations were then performed for the contact angles in the range $\theta_c = 95°$ and $\theta_c = 175°$ and the results are compared with the experimental data of Bisch et al. [3] and the theoretical predictions of Strani and Sabetta [23] in Fig. 2a where the frequency is plotted in the non-dimensional form defined as $\omega^* = \omega\sqrt{\frac{\rho_i R^3}{\gamma}}$. Note that the experimental data are extracted from Strani and Sabetta [23]. This figure shows that the Strani and Sabetta theory generally over predicts the oscillation frequency and the discrepancy between the computed and theoretical frequencies increases as the contact angle decreases. More importantly, the computational results are in a better agreement with the experimental data compared to the Strani and Sabetta theory especially for small contact angles, i.e., $\theta_c < 140°$, indicating the accuracy of the computational model.

After validating the computational results against the available experimental data, extensive simulations were then performed in order to examine the effects of governing non-dimensional parameters and fully characterize the small amplitude axisymmetric oscillations of viscous droplets on a flat substrate. Based on the experimental data of Jonas et al. [10] and considerations for the numerical stability and convergence of the numerical algorithm, we choose the set of non-dimensional parameters $\theta_c = 155°$, $\rho_i/\rho_o = 10$, $\mu_i/\mu_o = 10$, $Oh = 0.0465$ and $Bo = 0$ as the base case. Note that, for NaCl–Water droplet in air system studied by Jonas et al. [10], typical values are $\rho_i = 1144.7$ kg/m^3, $\rho_o = 1.23$ kg/m^3, $\mu_i = 1.36 \times 10^{-3}$ kg/m s, $\mu_o = 1.79 \times 10^{-5}$ kg/m s, $\gamma = 74.62$ mN/m, $R = 10$ μm and $\theta_c = 155°$, which corresponds to $\rho_i/\rho_o = 930$, $\mu_i/\mu_o = 76$, $Bo = 1.5 \times 10^{-5}$ and $Oh = 0.0465$. It is emphasized here that Jonas et al. [10] did not have any precise control on droplet size as droplets were generated by an ultrasonic nebulizer resulting in highly poly-dispersed droplets with a wide range of sizes. Therefore $R = 10$ μm is selected here as a representative droplet size rather than the exact value used in the experimental study. In the base case, the material properties of the droplet fluid, droplet radius and surface tension coefficient are set to the actual values of Jonas et al. [10] and the properties of the ambient fluid are set such that $\rho_i/\rho_o = \mu_i/\mu_o = 10$.

Computations were then performed for the base case in order to test the validity of the Strani and Sabetta theory for a liquid–gas system, e.g., NaCl–water droplet in air as studied experimentally by Jonas et al. [10]. The computational and theoretical results are plotted in Fig. 2b for the range of contact angles between $\theta_c = 95°$ and $\theta_c = 175°$ as before. It is clearly seen in this figure that there

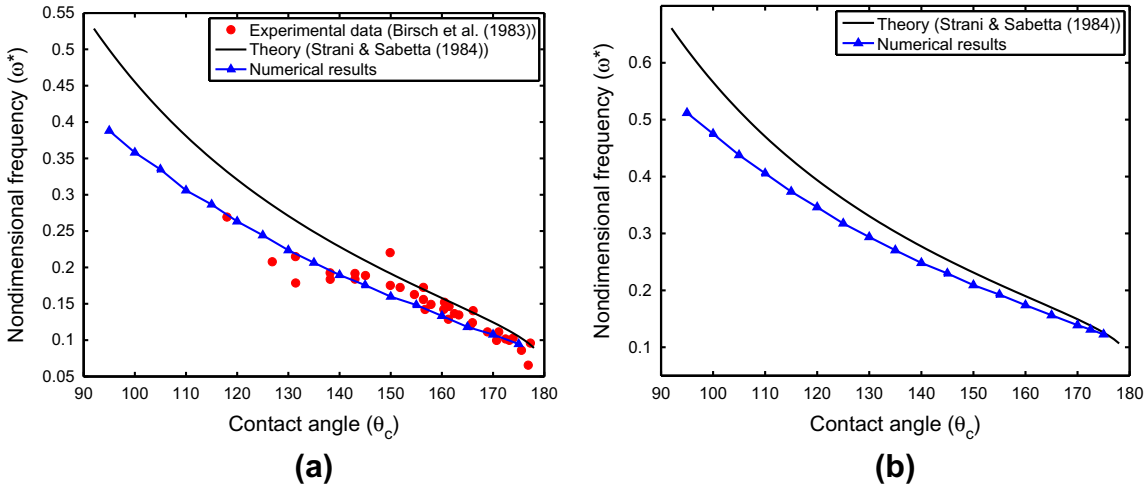

Fig. 2. Variation of free oscillation frequency with the contact angle. (a) For the liquid–liquid system studied experimentally by Bisch et al. [3]. The big dots indicate the experimental data taken form Bisch et al. [3] through Strani and Sabetta [24] ($\rho_i/\rho_o = 1$ and $\mu_i/\mu_o = 3.57$). (b) For the liquid droplet in a gas system studied experimentally by Jonas et al. [10], i.e., the base case.

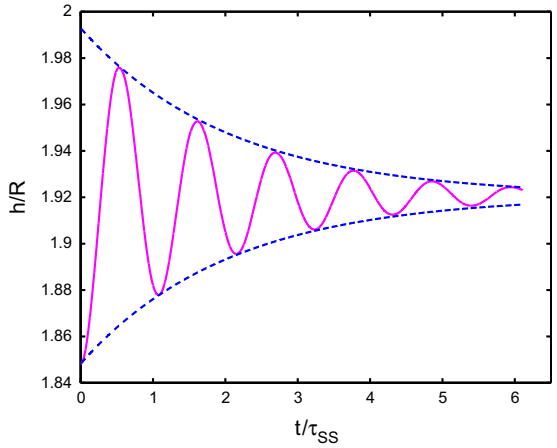

Fig. 3. Damped oscillations of the droplet height (solid line) for the base case. The dashed lines represent exponential damping fitted to the computational results in the form $\frac{h-h_{eq}}{h_i-h_{eq}} = e^{-\nu t}$ where h_{eq} is the equilibrium height, h_i is the initial height and ν is the damping rate determined by approximately fitting to the computational result ($\theta_c = 155°$, $\rho_i/\rho_o = 10$, $\mu_i/\mu_o = 10$).

is a good agreement between the computational and theoretical results for large contact angles but there is significant discrepancy for small contact angles similar to the liquid–liquid system. Fig. 2 shows that the Strani and Sabetta theory generally over predicts the oscillation frequency and difference between the computational and theoretical results increases as the contact angle decreases.

The time history of height of droplet for the base case is plotted in Fig. 3 to show the overall oscillatory behavior of the droplet. The time is normalized by the period obtained from the Strani and Sabetta theory, i.e., $\tau_{SS} = 1/\omega_{SS}$ where ω_{SS} is given by Eq. (1). In Fig. 3, the dashed lines represent exponential damping fitted to the computational results in the form

$$\frac{h - h_{eq}}{h_i - h_{eq}} = e^{-\nu t}, \tag{4}$$

where h_{eq} is the equilibrium height, h_i is the initial height and ν is the damping rate determined by approximately fitting this expression to the computational data. This figure shows that the initial perturbations decay exponentially in time due to viscous dissipation similar to the case of an isolated droplet [12]. It also shows that the Strani and Sabetta theory over predicts the oscillation frequency compared to the direct numerical simulation.

As can be seen in Eq. (1), Strani and Sabetta theory [23] predicts that the frequency scales as $\omega \sim R^{-3/2}\gamma^{1/2}\rho_i^{-1/2}$. We next examine the accuracy of these scalings through extensive simulations. Quantities are scaled using respective reference values of the base case to keep the quantities in a range since we're interested in scalings rather than the exact values. For this purpose, computations are first performed for a range of drop radii while keeping the other variables the same as in the base case and the results are plotted in Fig. 4a where a line is fitted to the numerical results using linear least squares method. The fitted line indicates that the slope is about -1.495 that is close to -1.5 showing the validity of scaling $\omega \sim R^{-3/2}$. Next surface tension is varied while keeping the other variables the same as the base case and the results are plotted in Fig. 4b where the linear least squares fit indicates a slope of 0.505 showing the validity of the scaling $\omega \sim \gamma^{1/2}$. Finally normalized frequency is plotted against normalized droplet density in Fig. 4c. The line fitted to the numerical data using a linear least squares method indicates approximate slope of -0.493 showing the validity of the scaling $\omega \sim \rho_i^{-1/2}$.

In the experimental study of Jonas et al. [10], NaCl–water droplet was excited in air to deduce the contact angle. In this system, the density and viscosity ratios are about 930 and 76, respectively. Therefore it is important to investigate effects of density and viscosity ratios on the free oscillation frequency of droplet in partial wetting with the substrate since the computational simulations have been performed for much smaller density and viscosity ratios to simulate a liquid droplet-gas system mainly due to numerical concerns. Fig. 5a and b respectively show the effects of the density and viscosity ratios on the oscillation frequency for the base case. It is seen in these figures that the effects of both density and viscosity ratios decrease rapidly and become insignificant after $\rho_i/\rho_i \geqslant 10$ and $\mu_i/\mu_o \geqslant 10$ verifying the assumption that free vibrations of a liquid droplet in a gas can be simulated using smaller density and viscosity ratios.

We finally examine the rate of damping due to viscous dissipation. The damping rate is normalized as $\nu^* = \nu\sqrt{\frac{\rho_i R^3}{\gamma}}$. Fig. 6a shows the variation of the normalized damping rate with the contact angle. It is emphasized here that computing damping rate involves

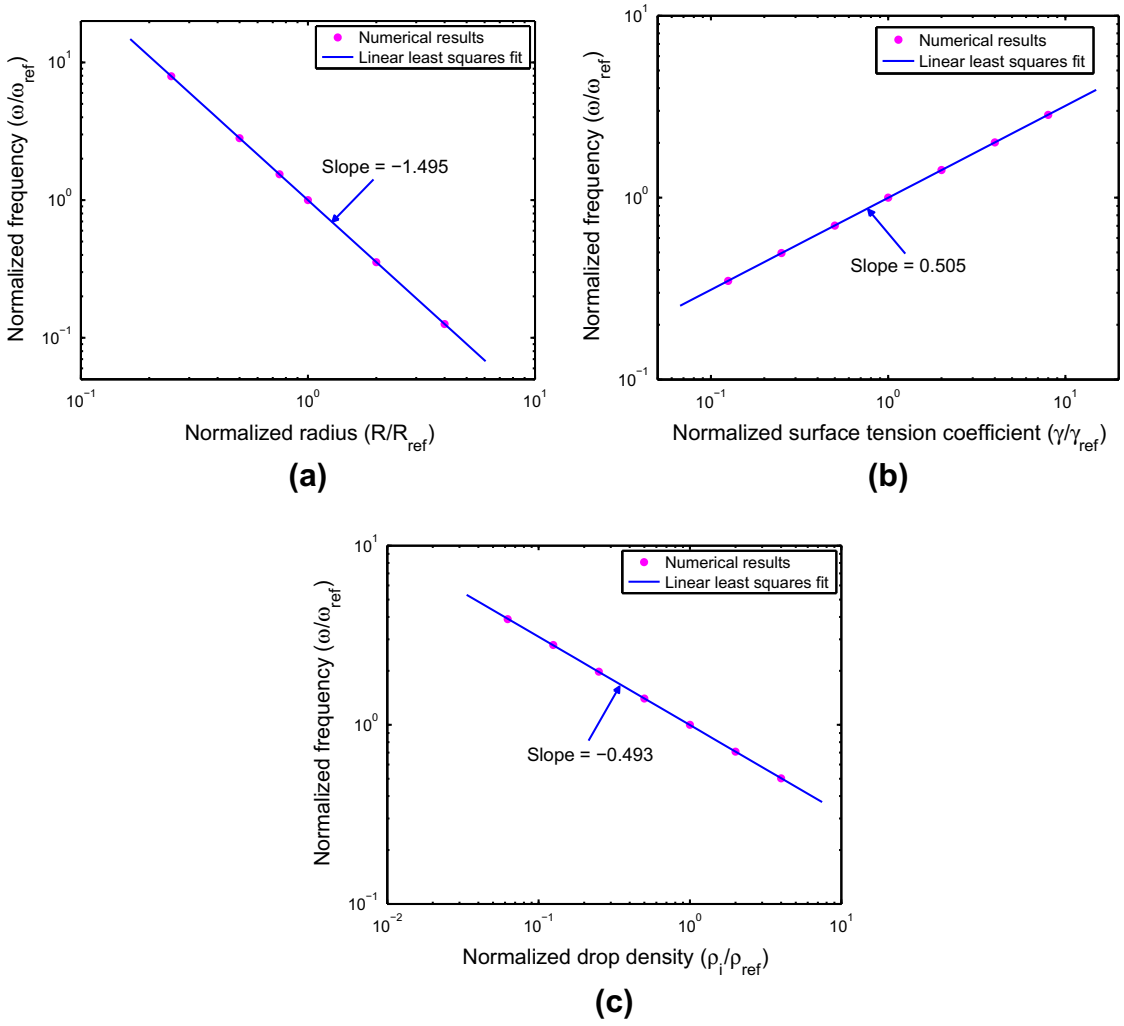

Fig. 4. Variation of free oscillation frequency with (a) the droplet radius, (b) surface tension coefficient and (c) the density of drop fluid. The solid lines are the linear least squares fits to the computational results (symbols).

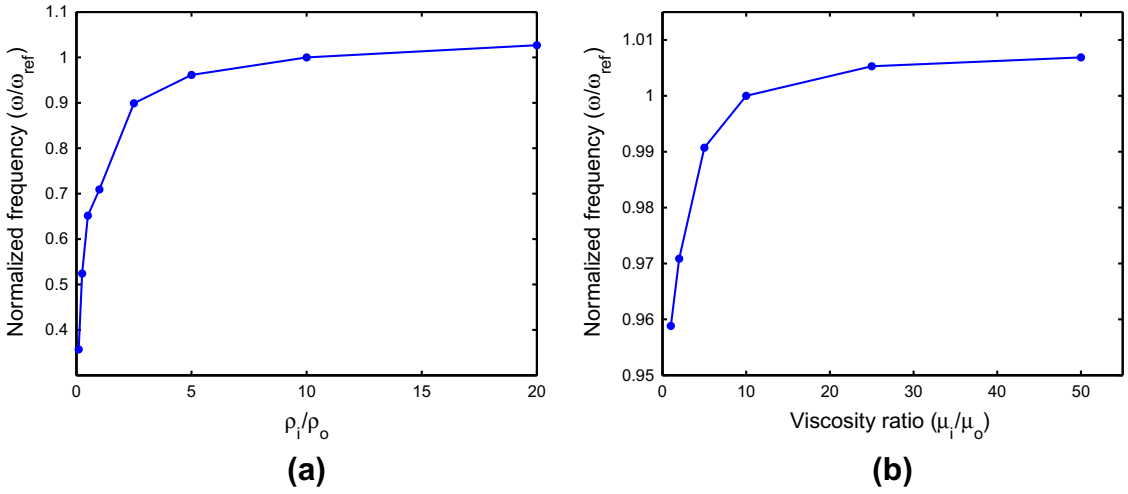

Fig. 5. Variation of free oscillation frequency with (a) the density and (b) the viscosity ratios.

likely more numerical error than the other quantities since it is computed indirectly by fitting an exponential function (Eq. (4)) to the time histories. The numerical error is expected to be significant especially for large contact angles, i.e., $\theta_c \geqslant 160°$. Nevertheless, Fig. 6a shows that the damping rate decreases with increasing contact angle, which is consistent with the theoretical

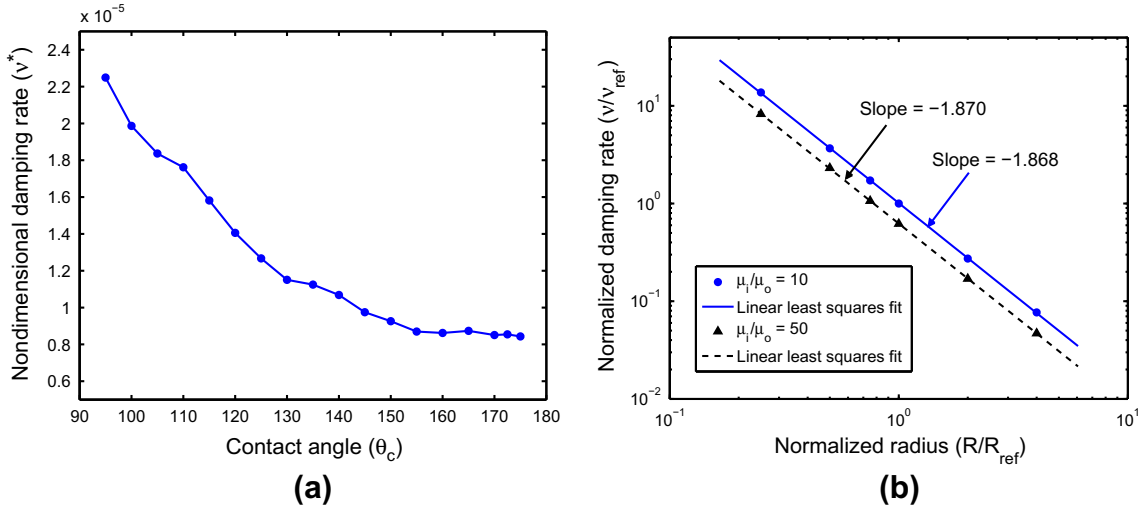

Fig. 6. (a) Variation of normalized damping rate with the contact angle. (b) Normalized damping rate against normalized droplet radius for viscosity ratios of $\mu_i/\mu_o = 10$ and $\mu_i/\mu_o = 50$. The lines are the linear least squares fits to the computational results (symbols).

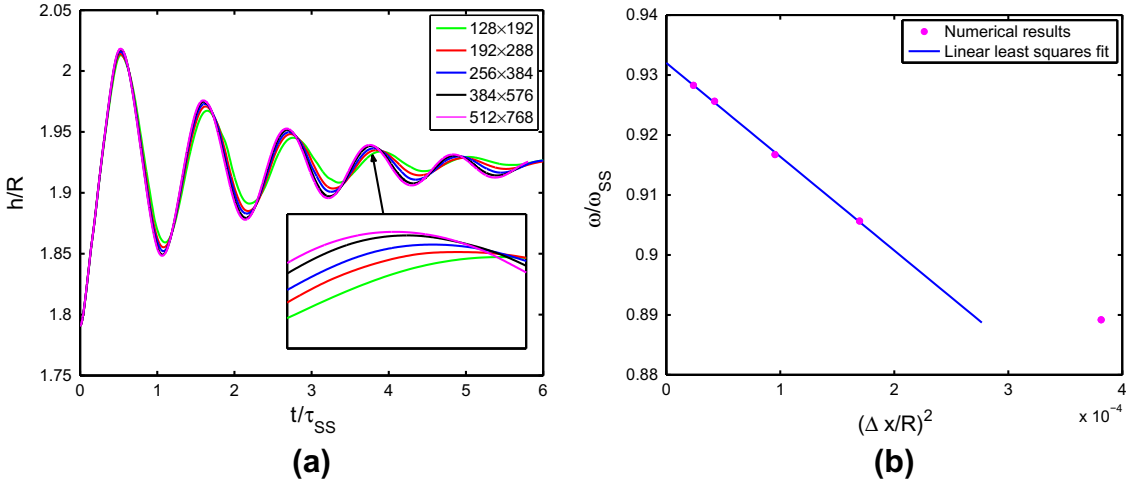

Fig. 7. Grid convergence of the numerical simulations for the base case. (a) The time histories of droplet height computed on the computational grids ranging between 128×192 and 512×768. (b) Variation of normalized free oscillation frequency with $(\Delta x/R)^2$. The solid line is the linear least squares fit to the computational results indicating the expected second order accuracy of the method.

predictions of Strani and Sabetta [24]. Computations are also performed to examine the effects of droplet size and the viscosity of ambient fluid on the viscous damping for over a range of droplet radii and two different viscosity ratios while keeping the other parameters the same as the base case. The results are plotted in Fig. 6b on a log–log scale. The lines are fitted to the computational results using linear least squares. This figure consistently shows that the damping rate scales as $v \sim R^{-1.87}$ for both viscosity ratios. In addition, the damping rate is larger for the smaller viscosity ratio mainly due to larger contribution of the ambient fluid.

4. Conclusions

Small amplitude free oscillations of a viscous droplet in partial contact with a flat substrate have been studied computationally using a front-tracking method. Extensive direct numerical simulations have been performed to examine the validity of Strani and Sabetta theory [23,24] and fully characterize the axisymmetric free surface oscillations of a supported droplet in an immiscible fluid. It is found that the Strani and Sabetta theory is valid for large contact angles but significantly deviates from the computational results as the contact angle decreases while the dependence of the oscillation frequency remains the same as predicted by the theory, i.e., $\omega \sim R^{-3/2}\rho_i^{-1/2}\gamma^{1/2}$. The effects of viscosity and density ratios decrease rapidly and become insignificant when $\rho_i/\rho_o \geqslant 10$ and $\mu_i/\mu_o \geqslant 10$. It is also found that the oscillations decay exponentially in time due to viscous dissipation similar to the case of an isolated droplet [12]. Viscous damping rate decreases with increasing contact angle and approximately scales with the droplet size as $v \sim R^{-1.87}$ irrespective of the viscosity ratio.

Acknowledgements

The authors are grateful to the Scientific and Technical Research Council of Turkey (TUBITAK) for support of this research through Grant 112M181 and Turkish Academy of Sciences through TUBA-GEBIP program. The first author (UO) is supported by TUBITAK through BIDEB. We thank Prof. Alper Kiraz, Dr. Alexandr Jonas and Yasin Karadag for bringing this problem to our attention and helpful discussions during the preparation of this paper.

Appendix A. Grid convergence

We briefly discuss here the grid convergence and accuracy of the computational results presented in the paper. For this purpose, series of simulations are performed for the base case using successively refined computational grids ranging between 128×192 and 512×768. The time histories of the normalized height of the droplet are plotted in Fig. 7a where the inset shows a blow out view of the results at about $t/\tau_{SS} = 4$. As can be seen in this figure, the difference between the results gets smaller as the grid is refined demonstrating the grid convergence. The normalized frequency is plotted in Fig. 7b as a function of $(\Delta x/R)^2$ where Δx is the grid size. Note that the grid sizes in the radial and axial directions are the same since uniform Cartesian grids are used in all the results presented in this paper. The linear least squares fit in Fig. 7b shows the expected second order spatial accuracy of the method. It also shows that it is sufficient to use a 384×768 grid to reduce the spatial discretization error below 1% for this case.

References

[1] Basaran OA. Nonlinear oscillations of viscous liquid drops. J Fluid Mech 1992;241:169–98.
[2] Basaran OA, DePaoli DW. Nonlinear oscillations of pendant drops. Phys Fluid 1994;6:2923.
[3] Bisch C, Lasek A, Rodot H. Hydrodynamic behavior of spherical semi-free liquid volumes in simulated weightlessness. J Mec Theor Appl 1982;1:165.
[4] B Bostwick J, Steen PH. Capillary oscillations of a constrained liquid drop. Phys Fluid 2009;21:032108-1–032108-10.
[5] Foote GB. A numerical method for studying liquid drop behavior: simple oscillation. J Comput Phys 1973;11(4):507–30.
[6] Ganan A, Barrero A. Free oscillations of liquid captive drops. Microgravity Sci Technol 1990;3:70–86.
[7] Harlow FH, Welch JE. Numerical calculation of time-dependent viscous incompressible flow of fluid with free surface. Phys Fluid 1965;8:2182.
[8] James AJ, Smith MK, Glezer A. Vibration-induced drop atomization and the numerical simulation of low-frequency single-droplet ejection. J Fluid Mech 2003;476:29–62.
[9] James AJ, Vukasinovic B, Smith MK, Glezer A. Vibration-induced drop atomization and bursting. J Fluid Mech 2003;476:1–28.
[10] Jonas A, Karadag Y, Tasaltin N, Kucukkara I, Kiraz A. Probing microscopic wetting properties of superhydrophobic surfaces by vibrated micrometer-sized droplets. Langmuir 2011;27(6):2150–4.
[11] Karadag Y, Jonas A, Tasaltin N, Kiraz A. Determination of microdroplet contact angles using electrically driven droplet oscillations. Appl Phys Lett 2011;98:194101.
[12] Kistler SF. Hydrodynamics of wetting. In: Berg JC, editor. Wettability. New York USA: Marcel Dekker; 1993.
[13] Lamb H. Hydrodynamics. Cambridge, (UK): Cambridge University Press; 1932.
[14] Lopez C, Hirsa A. Fast focusing using a pinned-contact liquid lens. Nat Photon 2008;2:610.
[15] Muradoglu M, Tasoglu S. A front-tracking method for computational modeling of impact and spreading of viscous droplets on solid walls. Comput Fluids 2010;39(4):615–25.
[16] Prosperetti A. Free oscillations of drops and bubbles: the initial-value problem. J Fluid Mech 1980;100:334–47.
[17] Prosperetti A. Linear oscillations of constrained drops, bubbles, and plane liquid surfaces. Phys Fluid 2012;24:032109-1–032108-15.
[18] Ramalingam SK, Basaran OA. Axisymmetric oscillation modes of a double droplet system. Phys Fluid 2010;22:112111.
[19] Ramalingam SK, Ramkrishna D, Basaran OA. Free vibrations of a spherical drop constrained at an azimuth. Phys Fluid 2012;24:082102.
[20] Rodot H, Bisch C, Lasek A. Zero-gravity simulation of liquids in contact with a solid surface. Acta Astronaut 1979;6:1083–92.
[21] Ruiz-Cabello FJM, Rodriguez-Valverde MA, Cabrerizo-Vilchez MA. Comparison of the relaxation of sessile drops driven by harmonic and stochastic mechanical excitations. Langmuir 2011;27(14):8748–52.
[22] Siekmann J, Schilling U. On the vibrations of an inviscid liquid droplet contacting a solid wall in a low-gravity environment. Appl Microgravity Technol 1989;2:17–26.
[23] Strani M, Sabetta F. Free vibrations of a drop in partial contact with a solid support. J Fluid Mech 1984;141:223–47.
[24] Strani M, Sabetta F. Viscous oscillations of a supported drop in an immiscible fluid. J Fluid Mech 1988;189:397–421.
[25] Tasoglu S, Kaynak G, Szeri AJ, Demirci U, Muradoglu M. Impact of a compound droplet on a flat surface: a model for single cell epitaxy. Phys Fluid 2010;22(8):082103.
[26] Theisen J, Davoust L. Dual-frequency electrowetting: application to drop evaporation gauging within a digital microsystem. Langmuir 2012;28(1):1041–8.
[27] Tryggvason G, Bunner B, Esmaeeli A, Juric D, Al-Rawahi N, Tauber W, et al. A front-tracking method for the computations of multiphase flow. J Comput Phys 2001;169(2):708–59.
[28] Unverdi SO, Tryggvason G. A front-tracking method for viscous, incompressible, multi-fluid flows. J Comput Phys 1992;100(1):25–37.
[29] Vukasinovic B, Smith MK, Glezer A. Dynamics of a sessile drop in forced vibration. J Fluid Mech 2007;587:395–423.
[30] Wilkes ED, Basaran OA. Forced oscillations of pendant (sessile) drops. Phys Fluid 1997;9:1512.
[31] Yamakita S, Matsui Y, Shiokawa S. New method for measurement of contact angle (droplet free vibration frequency method). Jpn J Appl Phys 1999;38:3127.